

## Particularities of C<sub>60</sub> Transformations at 1.5 GPa

**V. A. Davydov, L. S. Kashevarova, and A. V. Rakhmanina**

*Institute of High-Pressure Physics of the Russian Academy of Sciences, 142092, Troitsk, Moscow Region, Russian Federation*

**V. Agafonov,\* H. Allouchi, and R. Céolin**

*Laboratoire de Chimie Physique, Faculté de Pharmacie de l'Université de Tours, 31 av. Monge, 37200 Tours, France*

**A. V. Dzyabchenko**

*Karpov Institute of Physical Chemistry, ul. Obukha, 10, Moscow 107120, Russian Federation*

**V. M. Senyavin**

*Chemistry Department, Moscow State University, Moscow 119899, Russian Federation*

**H. Szwarc**

*Laboratoire de Chimie Physique des Matériaux Amorphes, UMR 8611, CNRS, Bâtiment 490, Université Paris XI, 91405, Orsay, France*

**T. Tanaka and K. Komatsu**

*Institute for Chemical Research, Kyoto University, Uji, Kyoto-fu 611, Japan*

*Received: May 19, 1998; In Final Form: October 19, 1998*

The high-pressure states of C<sub>60</sub> fullerene corresponding to the 1.5 GPa isobaric section of its  $p,T$  diagram in the 293–1073 K temperature range were investigated by X-ray diffraction and IR and Raman spectroscopies. It was shown that increasing the treatment temperature of C<sub>60</sub> at quasihydrostatic pressure changes the nature of the polymerization products. The IR and Raman spectra of the high-pressure materials obtained at 423 K are similar to the spectra of the dumb-bell-shaped C<sub>60</sub> dimer synthesized in a solid-state mechanochemical reaction of C<sub>60</sub> with potassium cyanide by Wang et al.<sup>1</sup> It can be concluded that this dumb-bell-shaped dimer is the main structural unit forming the low-pressure polymerization product. So, on further temperature increase, the dimer phase becomes unstable and transforms into the “low-pressure” orthorhombic polymerized phase of C<sub>60</sub> which, in turn, transforms into the tetragonal polymerized phase at temperatures above ~723 K. Depolymerization of the polymerized phases at temperatures above ~900 K results in the formation of the monomeric fcc phase of C<sub>60</sub> fullerene, which agrees with the experimental data determined previously by Bashkin et al.<sup>2</sup>

### Introduction

Investigations carried out in the past few years have led to the determination of the main features of the  $p,T$  diagram of C<sub>60</sub> fullerene. It has been shown that carbon states resulting from high-pressure–high-temperature treatments of C<sub>60</sub> can be qualitatively divided into three groups: (i) molecular (or monomeric), (ii) polymolecular (polymerized and polycondensed), and (iii) “atomic states”.<sup>3</sup> In the polymerized state domain, phases containing chains or layers of chemically bonded C<sub>60</sub> molecules were obtained by changing the treatment conditions.<sup>4–8</sup> One 1D and two 2D polymerized phases were observed: the orthorhombic (O),<sup>6,9–11</sup> the tetragonal (T),<sup>6,12</sup> and the rhombohedral (R).<sup>4–8,12</sup> The two latter phases can exist at high pressure up to approximately 1073 K; at higher temperatures they transform into an “atomic” material (hard amorphous carbon).<sup>8,12</sup> However, until now, the proposed descriptions have

not resulted in an equilibrium phase diagram in the conventional sense; they rather give mappings showing which high-pressure states are retained as metastable materials after fullerene has been treated at given  $p,T$  values then quenched to ambient conditions.<sup>13</sup> Full characterization of interconversions between normal and polymerized C<sub>60</sub> phases at different  $p,T$  conditions, especially regarding their existence ranges as well as their identification, was already discussed by Davydov et al.,<sup>10</sup> Sundqvist et al.,<sup>13</sup> and Marques et al.,<sup>14</sup> but it is still necessary to determine which high-pressure material is really stable at a given  $p,T$  point and which is metastable: only after this has been achieved will a true equilibrium phase diagram (if it exists) emerge.

The aim of the present study was to get a more accurate identification of polymerized phases found below 2.0 GPa by using different techniques: X-ray powder diffraction (XRD) and vibrational (IR and Raman) spectroscopies. To that purpose, the evolution of C<sub>60</sub> states at 1.5 GPa as a function of

\* To whom correspondence should be addressed.

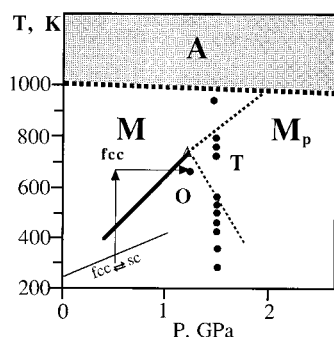


**Figure 1.** Fragment of  $p,T$  diagram of C<sub>60</sub> with experimental points at 1.5 GPa. A represents the existence range of atomic carbon materials. M corresponds to the monomeric state. Mp corresponds to the range of O and T polymerized phases of C<sub>60</sub>. ▲ represents the suggested triple point (fcc-O-T).

temperature and time was studied and the analysis of the structural relationships between the polymerized phases was performed.

### Experiment

Fullerene C<sub>60</sub> purchased from TermUSA (purity 99.9%) was sublimed twice in a vacuum at about 800 K to remove any remaining solvent. The treatment was performed inside the "Maxim" (a piston-cylinder type) and "toroid" devices. The experimental procedure consists in loading the samples up to the required pressure at room temperature, followed by heating at given temperature ( $\pm 3$  K according to chromel–alumel thermocouples) for 1–50 000 s. The high-pressure products of fullerite were conserved by quenching them down to room temperature under pressure and they were then studied at ambient conditions (the details were already discussed by Szwarc et al.<sup>15</sup>). XRD experiments were carried out by means of an INEL CPS120 position sensitive detector using the Cu K $\alpha_1$  radiation ( $\lambda = 1.5406$  Å). The powdered samples were introduced into 0.5 mm diameter Lindemann glass capillaries which were rotated around the  $\Theta$  axis during the experiments. A Bruker FT Raman RFS 100 spectrometer was used to record the spectra. The Nd:YAG laser was operated at 1064 nm with a 130 mW power. The IR transmission spectra of samples in KBr matrix were recorded with a Specord M80 spectrometer.

### Results and Discussion

The  $p,T$  parameters of all high-pressure experiments are plotted together with a fragment of the  $p,T$  diagram published previously by Davydov et al.<sup>3</sup> and Sundqvist.<sup>13</sup> In the diagram presented in Figure 1, region M corresponds to the monomeric molecular-crystalline state. Region Mp corresponds to the different polymerized phases of C<sub>60</sub> (in the present study, O and T). Region A (separated by a dotted line) is the region of existence of "atomic" carbon states resulting from the destruction of the C<sub>60</sub> molecular skeleton of monomeric fcc and polymerized phases. The upper solid line represents the phase equilibrium boundaries between the monomeric phases and the polymerized phases of C<sub>60</sub> for the range including  $\sim 400$ – $700$  K and  $0.4$ – $1.2$  GPa as determined by Bashkin et al.<sup>2</sup> This line is continued by a dotted line using the present experimental data. Other explanations are given in the text below.

**a. XRD Study.** Figure 2 presents the evolution of the XRD patterns of the samples obtained at 1.5 GPa when temperature changes. In the low-temperature region (298–423 K), the patterns of samples treated for as long as 1000 s mainly keep cubic characteristics except some asymmetric broadening and

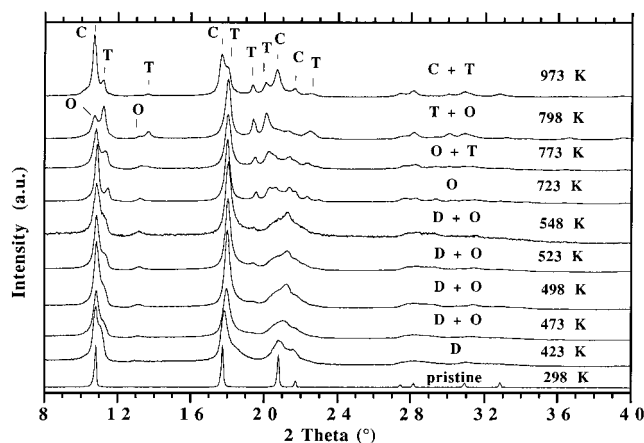


**Figure 2.** Evolution of the XRD patterns as a function of temperature (1000 s of treatment).

a slight shift of the peaks toward greater angles (Figure 2). However, a prolonged heating for 10 000 s leads to more pronounced changes: (1) cubic peaks (111) and (220) begin to split into two lines, and (2) a new diffuse peak appears at  $12^\circ$ – $13^\circ$  ( $2\Theta$ ).

A similar phenomenon has been observed at low pressures and temperatures by Persson et al.,<sup>16</sup> who also noted that polymer formation depends on the time of treatment.

However, the treatment of a sample at a higher temperature during a short period is equivalent to the action of a lower temperature during a long period. For example, the same changes as above in the XRD patterns were obtained after 1000 s of treatment in the temperature range extending to 548 K. An accurate indexation of the patterns in these conditions is not possible, but it can be understood in terms of a slightly distorted cubic lattice with orthorhombic parameters ( $a = 14.2$  Å,  $b = 9.9$  Å,  $c = 9.4$  Å), similar to those obtained for the "high-pressure" orthorhombic phase by Nunez-Regueiro et al.<sup>6</sup> However, using spectroscopic methods only, we could show that the above-mentioned products contain a mixture of dimers and polymeric chains of C<sub>60</sub>. Therefore, they cannot be considered as a single phase. Increasing the temperature from 548 to 723 K leads to less broad and more intense XRD peaks. At 723 K after heating for 1000 s, the formation of the "low pressure" orthorhombic phase (O)<sup>9</sup> was detected. The unit cell parameters of this phase [ $a = 9.086(4)$  Å,  $b = 9.807(7)$  Å,  $c = 14.73(1)$  Å] are in agreement with previous determinations.<sup>9–11</sup>

The treatment for a long time (10 000 s) at 723 K as well as the treatment for a short time (1000 s) at 773 K lead to the formation of a mixture of phase O with another phase indexed as tetragonal (T) [ $a = 9.083(5)$  Å,  $c = 15.00(2)$  Å] (some reflections are marked T in Figure 2). This phase is identical with the tetragonal one reported before as forming at higher pressure.<sup>6,12</sup> Our attempts to prepare pure phase T by treatment for a long time (10 000 s) at 798 K were unsuccessful: in all experiments, besides the main phase T, some amount of phase O was also detected. However, the preparation of pure phase T is possible at 2.3 GPa and was described by Davydov et al.<sup>17</sup>

Note that the identification of these mixtures through XRD analysis alone can be misleading because of the similarity of the XRD patterns of mixtures O + T and R + T in the  $8$ – $40$  ( $2\Theta$ ) range. Thus, at similar pressures and temperatures, XRD patterns were thought to indicate the presence of mixtures of phases R and T<sup>18</sup> or of phases O, T and R.<sup>19,20</sup> In the present work, IR spectral data confirm the presence of phases O and T but fail to reveal the existence of phase R.

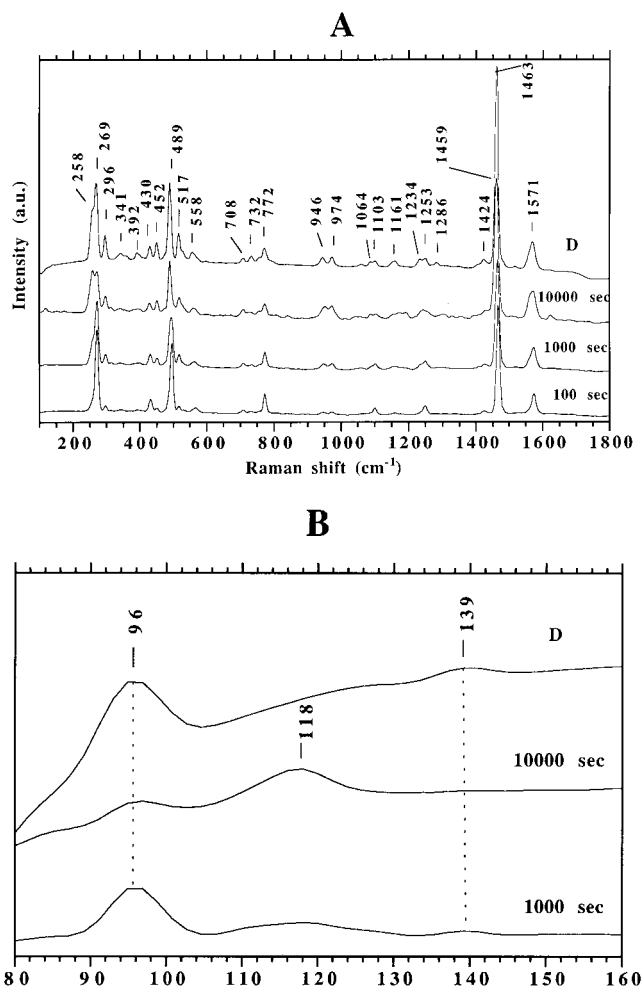
After treatment at 973 K (1000 s), the sample also contains two phases: the main one was found to be fcc, with a lattice parameter equal to 14.17(1) Å (C peaks in Figure 1) and the other phase is identical to phase T. We suggest that this phenomenon is due to the depolymerization of polymerized phases (O and T) which results in the formation of the monomeric fcc phase of C<sub>60</sub>. This is in agreement with the value of the experimental  $dT/dP$  slope of the equilibrium line between the monomeric fcc phase and the polymerized states of the system as determined by Bashkin et al.<sup>2</sup> The presence of some amount of phase T within the fcc one can be explained by too slow a quenching rate from the treatment temperature of the samples. The formation of phase T during a long heating of phase O at 723 K and during the cooling of fcc C<sub>60</sub> from 973 K indicates that phase T should be the more stable polymerized state at 1.5 GPa in the 723–900 K range. The stability range of phase O is lying at lower pressure (1.0–1.2 GPa).<sup>11,16</sup> Moreover, phase O was prepared using another path: by loading pristine C<sub>60</sub> at room temperature up to 0.5 GPa, heating it up to 673 K at constant pressure, then increasing pressure up to 1.2 GPa (with the temperature maintained at 673 K), and, finally, keeping the sample at 1.2 GPa and 673 K for 10 000 s (see arrow in Figure 1). In this way, phase O is obtained directly from the monomeric fcc phase.

These results suggest that the  $p,T$  phase diagram of C<sub>60</sub> has a triple point (fcc–O–T) near 720 K and 1.2 GPa (marked by ▲ in Figure 1). The two dashed lines correspond (1) to the thermal stability limits of C<sub>60</sub> molecules in the monomeric and polymerized phases (upper line) and (2) to the supposed equilibrium line between the O and T phases. The latter line is approximate and more investigations are necessary to refine its  $p,T$  coordinates because of hysteresis phenomena.

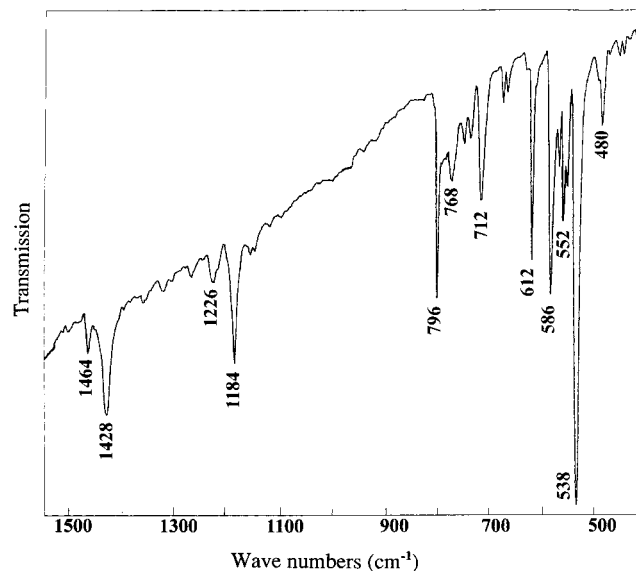
**b. Vibrational Spectroscopy.** As already mentioned, FT-Raman and IR spectroscopies were also used. They lead to reliable conclusions, especially for the samples treated at low temperature (293–423 K).

Figure 3A shows the evolution of the FT-Raman spectra of the samples synthesized at 423 K as a function of treatment time. After 100–1000 s treatments, the A<sub>g</sub>(2) line shift from 1468 to 1463 cm<sup>-1</sup> and all H<sub>g</sub> modes are split. Some new bands (at 946 and 974 cm<sup>-1</sup> and particularly the band at 96 cm<sup>-1</sup>, shown separately in Figure 3B) appear which cannot be viewed as H<sub>g</sub>-derived modes. The observed Raman spectrum is found to be identical with that of the dimer (identified here by C<sub>60</sub> = C<sub>60</sub>) synthesized in a solid-state mechanochemical reaction of C<sub>60</sub> with potassium cyanide by Wang et al.<sup>1</sup> (spectrum D in Figure 3, A and B) and more recently with lithium by Lebedkin et al.<sup>25</sup> The low-frequency band is close to the theoretically predicted interball vibration frequencies of the dumb-bell-shaped [2+2] C<sub>60</sub> dimer molecule.<sup>26–28</sup> However, after a 10 000 s treatment, the A<sub>g</sub>(2) line shifts to 1459 cm<sup>-1</sup> and new weak bands at 118 and 1620 cm<sup>-1</sup> appear. We suggest that at this moment the C<sub>60</sub> dimers begin to transform into 1D chains forming phase O. The almost pure O phase which appears after heating for 50 000 s at 423 K supports this assumption.

The IR spectrum of the 423 K–1000 s sample is given in Figure 4. In addition to F<sub>1u</sub>-derived modes, many new bands are observed in the spectrum, the more intense ones being those at 1464, 796, 768, 712, 612, 552, and 480 cm<sup>-1</sup>. These differences from the spectra of pristine C<sub>60</sub><sup>22</sup> clearly indicate that inter-ball linkage occurs even under these soft treatment conditions. Comparable spectral changes were found earlier in low-pressure treated<sup>12,16</sup> and phototransformed C<sub>60</sub>.<sup>23,24</sup> The IR spectrum of the sample is similar to that of the synthetic dimer



**Figure 3.** FT Raman spectra of samples obtained at 423 K as a function of time in comparison with that obtained from chemically synthesized [2 + 2] dimer (D spectrum). (A) 150–1800 cm<sup>-1</sup> range, (B) 80–160 cm<sup>-1</sup> range.



**Figure 4.** IR spectrum of a sample containing pressure-induced C<sub>60</sub> dimers (423 K, 1000 s).

and to the spectra of photoproducts interpreted recently by Esfarjani et al.<sup>29</sup> as composed of C<sub>60</sub> dimers too. Moreover, the IR spectra proved to be very sensitive to the presence of dimer and showed that the latter forms in observable amounts at 1.5 GPa even at room temperature after 1000 s or after 1 s at 423



K. Therefore, it may be concluded that the formation of the dumb-bell-shaped C<sub>60</sub>=C<sub>60</sub> is the first step of low-temperature high-pressure polymerization of C<sub>60</sub>. However, the existence of the pure high-pressure dimeric phase at temperatures lower than 423 K is still to be ascertained.

**c. Structural Relationship between Dimers, O and T Phases.** In this paragraph we mean to explain (i) why the dimer product leads to a disordered fcc phase of C<sub>60</sub> and (ii) how dimers may be transformed into chains which, in turn, transform into tetragonal layers.

The observed XRD spectra of dimerized C<sub>60</sub> can be interpreted in terms of a disordered fcc lattice in which each C<sub>60</sub> molecule is shifted from its exact position in the direction of one of its 12 nearest neighbors to form a dimer molecule. Since the magnitude of such a shift ( $\sim 0.5$  Å) is not large with respect to the cubic lattice parameter ( $\sim 14$  Å), the resulting arrangement of C<sub>60</sub> centers remains close to that of the parent fcc lattice. As a first approximation, it can be assumed that the various displacement vectors of the C<sub>60</sub> molecules occur along the 12  $\langle 110 \rangle$  cubic directions thus retaining a statistical mean cubic geometry. However, such displacements should entail some structural relaxation and the molecules will move to slightly different (less symmetrical) but energetically preferable positions. This results in differently oriented domains, so that initial orientation preferences of the dimeric molecules in the bulk substance are retained. Thus the dimer structure should deviate from the perfect fcc lattice, and moreover the different orientations of the dimers should generate defects such as stacking faults between domains. These faults will result in an overall lowering of symmetry and this should be the origin of the asymmetric peak broadening observed in the XRD patterns.

To support this model, we performed optimal packing calculations for C<sub>60</sub>=C<sub>60</sub> molecules. The crystal lattice energy calculated with an empirical intermolecular potential was minimized with respect to the crystal lattice and molecular rigid-body parameters (see refs 21 and 30 for the computation procedure). The starting models were constructed on the basis of the fcc arrangement of C<sub>60</sub> molecules—by grouping them in pairs in different ways to form the dimers with different orientations. As a result of the test, several crystal packings of various symmetries were found. [A full paper with the detailed calculation procedure and comparison of the obtained crystal structures of C<sub>60</sub>=C<sub>60</sub> will be presented elsewhere.] The most energetically stable structure was calculated to have monoclinic symmetry ( $P2_1/a$ ,  $a = 17.0$  Å,  $b = 9.7$  Å,  $c = 19.0$  Å,  $\beta = 123^\circ$ ) with geometrical parameters similar to those of the K-(Rb)-containing single-bonded C<sub>60</sub>-C<sub>60</sub> dimer structure<sup>31</sup> (in spite of different bond types between the two C<sub>60</sub> moieties inside the dimer units).

The dimer structure was found to be similar to that of the chain-containing O phase as far as the positions and orientations of C<sub>60</sub> units are concerned. In particular, the dimer molecules pack along linear chains within which obviously the double bonds of two neighboring dimers have the same orientation. This orientation means that the geometrical conditions for the formation of new [2+2] chemical bonds are fulfilled and the dimers should be able to link directly into infinite chains. This gives obvious structural reasons for considering the dimer phase as an intermediate to phase O.

A mechanism for the O  $\rightarrow$  T transformation observed at 3–8 GPa has been proposed previously by Marques et al.<sup>8</sup> It consists of weak displacement of chains (*Immm*) into tetragonal (*Immm*) layers. This mechanism, together with the structure of the so-called “high-pressure” orthorhombic phase, has already been

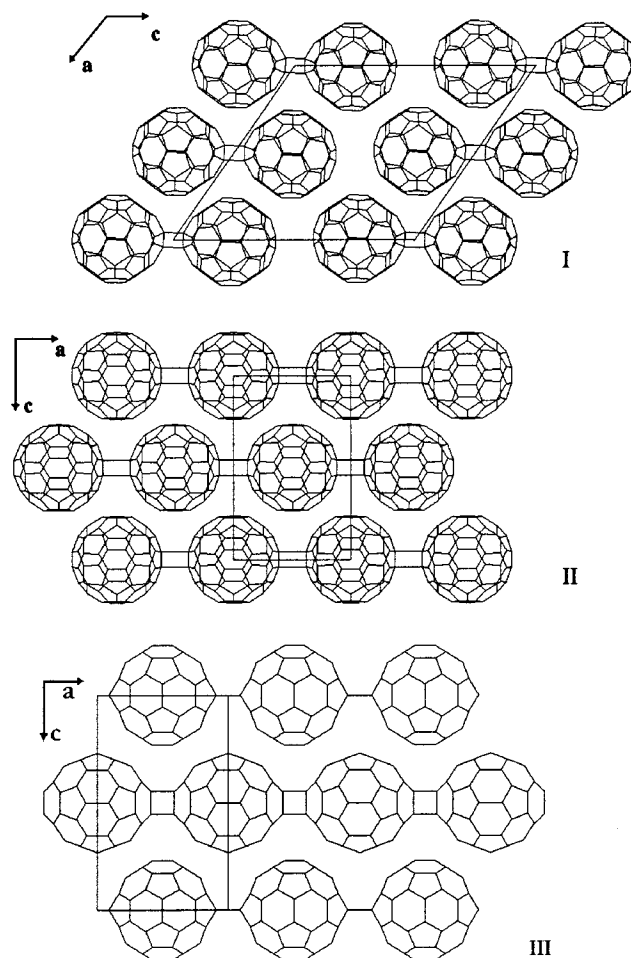


**Figure 5.** A comparison of the monoclinic dimer (I), phase O (II), and phase T (III) structures.

disputed by Agafonov et al.,<sup>9</sup> Davydov et al.,<sup>10</sup> and Moret et al.<sup>11</sup> We already discussed the structures of O and T.<sup>21</sup> In contrast with the model of *Immm* symmetry<sup>6</sup> (with a chain rotation angle  $\psi = 90^\circ$ ) for the orthorhombic phase (O), a *Pnnm* model, with the chains rotated from the *mmm* symmetrical orientation by  $\psi = 29^\circ$ , was suggested. Then, the pseudotetragonal *Immm* model of phase T,<sup>6</sup> with tetragonal layers packed on one another through a volume-centering translation, was replaced by a perfectly tetragonal *P4<sub>2</sub>/mmc* model, with adjacent layers related through the 4<sub>2</sub> screw axis. This means that the O  $\rightarrow$  T transformation cannot occur through a simple translation of the polymeric chains in the orthorhombic structure but needs the full reorientation of C<sub>60</sub> units, which is impossible without *breaking down* intermolecular bonds: therefore, it should require a high activation energy. This could explain the very low rate of O  $\rightarrow$  T transformation in the present conditions. The crystal structures of monoclinic dimer, phase O, and phase T are compared in Figure 5 (I, II and III), respectively.

## Conclusion

To conclude, XRD, Raman, and infrared measurements showed that treatment of C<sub>60</sub> at 1.5 GPa results, even at room temperature, in the formation of dumb-bell-shaped C<sub>60</sub>=C<sub>60</sub> dimers. The observed XRD spectra of dimerized C<sub>60</sub> present a disordered fcc lattice. This must be taken into account for the interpretation of the previously obtained results concerning the fcc  $\rightarrow$  sc transformation under high pressure. Thus, two types of transformations are possible when pressure is applied to C<sub>60</sub>

at room temperature: (i) a first-order transition induced by long-range orientational order between the  $C_{60}$  molecules ( $Fm\bar{3}m \rightarrow Pa\bar{3}$  transition) and (ii) a chemical reaction leading to the dumb-bell-shaped  $C_{60}=C_{60}$  dimer.

On increasing temperature, the  $C_{60}=C_{60}$  molecules combine into linear chains (phase O). These chains, in turn, transform very slowly into tetragonal layers of polymerized  $C_{60}$  (phase T).

Our results indicate that phase T should be the more stable polymerized state at 1.5 GPa in the 723–900 K range.

A tentative  $p,T$  diagram of  $C_{60}$  is presented. However, it is obvious that an exact determination of the phase equilibrium lines between different polymerized phases will require further studies because of the significant hysteresis of these phase transitions. However, if our diagram were right, this means that phases O and T could be obtained through different paths and the mechanism of their formation would depend on the  $p,T$  conditions of synthesis. For example, phase O should be obtained through the formation of dimers, or directly from the fcc phase of  $C_{60}$ , or from phase T.

**Acknowledgment.** The present work was supported by INTAS, Grant No. 93-2133, and by the Russian Fondation for Basic Research, Grant No. 97-03-33584a. We thank Prof. P. Dubois and Dr. I. Shourpa (Laboratoire de Chimie Analytique de la faculté de Pharmacie de Tours) for their help in recording the Raman spectra.

## References and Notes

- (1) Wang, G.-W.; Komatsu, K.; Murata, Y.; Shiro, M. *Nature* **1997**, *387*, 583. See also: Komatsu, K.; Wang, G.-W.; Murata, Y.; Shiro, M. *Fullerenes. Recent Advances in the Chemistry and Physics of Fullerenes and Related Materials*; Kadish, K. M., Ruoff, R. S., Eds.; The Electrochemical Society, Pennington, NJ, 1994; Vol. 4, p 290.
- (2) Bashkin, I.; Rashchupkin, V.; Gurov, A.; Moravsky, A.; Rybchenko, O.; Kobelev, N.; Soifer, Y.; Ponyatovsky, E. *J. Phys.: Condens. Mater.* **1994**, *6*, 7491.
- (3) Davydov, V. A.; Kashevarova, L. S.; Rakhmanina, A. V.; Ceolin R.; Szwarc, H. *JETP Lett.* **1996**, *63*, 818.
- (4) Iwasa, Y.; Arima, T.; Fleming, R. M.; Siegrist, T.; Zhou, O.; Haddon, R. C.; Rothberg, L. J.; Lyons, K. B.; Carter Jr., H. L.; Hebard, A. F.; Tycko, R.; Dabbagh, G.; Krajewski, J. J.; Thomas, G. A.; Yagi, T. *Science* **1994**, *264*, 1570.
- (5) Oszlanyi, G.; Forro, L. *Solid State Commun.* **1995**, *93*, 265.
- (6) Nunez-Regueiro, M.; Marques, L.; Hodeau, J.-L.; Berthoux, O.; Perroux, M. *Phys. Rev. Lett.* **1995**, *74*, 278.
- (7) Chun Hui Xu; Scuseria, G. E. *Phys. Rev. Lett.* **1995**, *74*, 274.
- (8) Marques, L.; Hodeau, J.-L.; Nunez-Regueiro, M.; Perroux, M. *Phys. Rev. B* **1996**, *54*, R12633.
- (9) Agafonov, V.; Davydov, V. A.; Kashevarova, L. S.; Rakhmanina, A. V.; Kahn-Harari, A.; Dubois, P.; Ceolin, R.; Szwarc, H. *Chem. Phys. Lett.* **1997**, *267*, 193.
- (10) Davydov, V. A.; Kashevarova, L. S.; Rakhmanina, V.; Dzyabchenko, A.; Agafonov, V.; Dubois, P.; Ceolin, R.; Szwarc, H. *JETP Lett.* **1997**, *66*, 120.
- (11) Moret, R.; Launois, P.; Persson, P.-A.; Sundqvist, B. *Europhys. Lett.* **1997**, *40*, 55.
- (12) Davydov, V. A.; Kashevarova, L. S.; Rakhmanina, A. V.; Agafonov, V.; Ceolin, R.; Szwarc, H. *Carbon* **1997**, *35*, 735.
- (13) Sundqvist, B. *Phys. Rev. B* **1998**, *57*, 3164. See also: Sundqvist, B. Fullerenes under high pressures, to be published in *Adv. Phys.*
- (14) Marques, L.; Hodeau, J.-L.; Nunez-Regueiro, M.; Perroux, M. *Phys. Rev. B* **1998**, *57*, 3166.
- (15) Szwarc, H.; Davydov, V. A.; Plotianskaya, S. A.; Kashevarova, L. S.; Agafonov, V.; Ceolin, R. *Synth. Met.* **1995**, *77*, 265.
- (16) Persson, P.-A.; Edlund, U.; Jacobsson, P.; Jonels, D.; Soldatov, A.; Sundqvist, B. *Chem. Phys. Lett.* **1996**, *258*, 540.
- (17) Davydov, V. A.; Kashevarova, L. S.; Rakhmanina, A. V.; Agafonov, V.; Allouchi, H.; Ceolin, R.; Dzyabchenko, A. V.; Senyavin, V. M.; Szwarc, H. *Phys. Rev. B* **1998**, *58*, 14786.
- (18) Blank, V. D.; Buga, S. G.; Dubitsky, G. A.; Serebryanaya, N. R.; Popov, M. Yu.; Sundqvist, B. *Carbon* **1998**, *36*, 319.
- (19) Rao, A. M.; Eklund, P. C.; Hodeau, J.-L.; Marques, L.; Nunez-Regueiro, M. *Phys. Rev. B* **1997**, *57*, 4766.
- (20) Rao, A. M.; Eklund, P. C.; Venkateswaran, U. D.; Ticker, J.; Duncan, M. A.; Bende, G. M.; Stephens, P. W.; Hodeau, J.-L.; Marques, L.; Nunez-Regueiro, M.; Bashkin, I. O.; Ponyatovsky, E. G.; Moravsky, A. P. *Appl. Phys. A* **1997**, *64*, 231.
- (21) Davydov, V. A.; Agafonov, V.; Dzyabchenko, A. V.; Ceolin, R.; Szwarc, H. *J. Solid State Chem.* **1998**, *141*, 164.
- (22) Martin, M. C.; Du, X.; Kwon, J.; Mihaly, L. *Phys. Rev. B* **1994**, *50*, 173.
- (23) Rao, A. M.; Zhou, P.; Wang, K.-A.; Hager, G. T.; Holden, J. M.; Wang, Y.; Lee, W.-T.; Bi, X. X.; Eklund, P. C.; Cornett, D. S.; Duncan, M. A.; Amster, I. J. *Science* **1993**, *259*, 955.
- (24) Burger, B.; Winter, J.; Kuzmany, H. Z. *Phys. B* **1996**, *101*, 227.
- (25) Lebedkin, S.; Gromov, A.; Giesa, S.; Gleiter, R.; Renker, B.; Rietschel, H.; Krätschmer, W. *Chem. Phys. Lett.* **1998**, *285*, 210.
- (26) Adams G. B.; Page, J. B.; Sankey, O. F.; O'Keeffe, M. *Phys. Rev. B* **1994**, *50*, 17471.
- (27) Porezag, D.; Pederson, M. R.; Frauenheim, Th.; Kohler, Th. *Phys. Rev. B* **1995**, *52*, 14963.
- (28) Kurti, J.; Nemeth, K. *Fullerene Sci. Technol.* **1997**, *5*, 429.
- (29) Esfarjani, K.; Hashi, Y.; Onoe, J.; Takeuchi, K.; Kawazoe, Y. *Phys. Rev. B* **1998**, *57*, 223.
- (30) Dzyabchenko, A. V.; D'yachkov, P. N.; Agafonov, V. *Russ. Chem. Bull.* **1995**, *44*, 1408.
- (31) Oszlanyi, G.; Bortel, G.; Faigel, G.; Granasy, L.; Bende, G. M.; Stephens, P. W.; Forro, L. *Phys. Rev. B* **1996**, *54*, 11849.